






## Article

# Simulation and Exergoeconomic Analysis of a Trigeneration System Based on Biofuels from Spent Coffee Grounds

Diana L. Tinoco Caicedo <sup>1,2,\*</sup> , Myrian Santos Torres <sup>2</sup> , Medelyne Mero-Benavides <sup>2</sup> , Oscar Patiño Lopez <sup>2</sup> , Alexis Lozano Medina <sup>3</sup> and Ana M. Blanco Marigorta <sup>3</sup> 

<sup>1</sup> Centro de Energías Renovables y Alternativas (CERA), Escuela Superior Politécnica del Litoral Ecuador, Guayaquil 090903, Ecuador

<sup>2</sup> Facultad de Ciencias Naturales y Matemáticas (FCNM), Escuela Superior Politécnica del Litoral Ecuador, Guayaquil 090903, Ecuador

<sup>3</sup> Department of Process Engineering, Universidad de Las Palmas de Gran Canaria, 35017 Las Palmas de Gran Canaria, Spain

\* Correspondence: dtinoco@espol.edu.ec

**Abstract:** Biofuels have become a source of renewable energy to offset the use of fossil fuels and meet the demand for electricity, heat, and cooling in the industrial sector. This study aims to (a) develop a simulation of a trigeneration system based on a gas turbine cycle and an absorption chiller unit, using biomass and syngas from spent coffee grounds (SCGs) to replace the conventional system currently supplying the energy requirements of an instant coffee plant located in Guayaquil, Ecuador, and (b) carry out an exergoeconomic analysis of the simulated system to compare the effects of different fuels. The results showed an increase in the exergetic efficiency from 51.9% to 84.5% when using a trigeneration system based on biomass instead of the conventional non-integrated system. Furthermore, the biomass-based system was found to have the lowest operating costs (\$154.7/h) and the lowest heating, cooling, and power costs (\$10.3/GJ, \$20.2/GJ, and \$23.4/GJ, respectively). Therefore, the results of this analysis reveal that using SCGs as biofuel in this instant coffee plant is feasible for producing steam, chilled water, and power.

**Keywords:** syngas; biomass; spent coffee grounds; trigeneration system; exergy destruction cost rate



**Citation:** Tinoco Caicedo, D.L.; Santos Torres, M.; Mero-Benavides, M.; Patiño Lopez, O.; Lozano Medina, A.; Blanco Marigorta, A.M. Simulation and Exergoeconomic Analysis of a Trigeneration System Based on Biofuels from Spent Coffee Grounds. *Energies* **2023**, *16*, 1816. <https://doi.org/10.3390/en16041816>

Academic Editor: Vladislav A. Sadykov

Received: 9 January 2023

Revised: 1 February 2023

Accepted: 9 February 2023

Published: 11 February 2023



**Copyright:** © 2023 by the authors. Licensee MDPI, Basel, Switzerland. This article is an open access article distributed under the terms and conditions of the Creative Commons Attribution (CC BY) license (<https://creativecommons.org/licenses/by/4.0/>).

## 1. Introduction

Around the world, it is estimated that 14% of factories use trigeneration systems (CCHP) to provide services for their production processes [1]. However, in Ecuador, the factories still use non-integrated systems based on fossil fuels (vapor compression cycles and power generators), which has become a serious economic and environmental problem, especially for energy-intensive processes, such as instant coffee production.

The production process of instant coffee requires vast amounts of steam, chilled water, and electricity for unit operations such as coffee extraction, evaporation, spray drying, and lyophilization. At the same time, this process generates approximately 40% of its raw material as spent coffee grounds (SCGs), which is an agro-industrial waste that has the potential to be converted into different biofuels; however, it is discarded in landfills. Currently, different organic wastes generated in factories have been studied as a source of biofuels [2–4], specially syngas. Sadi et al. [5] concluded that the use of sugarcane bagasse as biofuel for heating and cooling systems is economically and environmentally feasible. In addition, they demonstrated that other organic waste such as prosopis, wood chips, and rice husks [6] could be used in large-scale cooling systems. Abdel et al. [7] determined that it is economically feasible to use municipal solid waste for power generation in Saudi Arabia.

Giuliano et al. [8] proposed the use of digestate-derived syngas to produce dimethyl ether from municipal solid waste. The results highlighted the importance of H<sub>2</sub>/CO/CO<sub>2</sub> ratios in order to optimize the process.

Sofia et al. [9] demonstrated the technical and economic feasibility of an Integrated Gasification Combined Cycle for power generation using a mixture of olive husks and grape seed meal. They found that the use of syngas reduced emissions by 16% compared to the system fueled by coal and petcoke.

Exergy-based methods are useful for evaluating the performance of energy conversion systems because they integrate the first and second laws of thermodynamics. The exergy analysis allows the allocation and quantification of the irreversibilities (exergy destruction rate) of a system. Furthermore, the exergoeconomic analysis is a method that combines exergy analysis with economic analysis. The method determines the cost of thermodynamic inefficiencies in a system [10].

Some exergy and exergoeconomic analyses have been performed on biofuel-based power generation systems in order to evaluate how to increase the exergetic efficiency and reduce operational costs.

Wu et al. [11] performed an exergoeconomic analysis on a CCHP system coupled with biomass–steam gasification assisted by solar heat. The exergy analysis results show that the exergy efficiency of the system is higher in the heating mode than in the cooling mode. They also identified that the internal combustion engine caused 49.2% of the overall exergy destruction and loss.

Gholizadeh et al. [12] performed an exergoeconomic analysis on a cooling/electricity cogeneration system based on an organic Rankine cycle (ORC), an ejector cooling cycle (ECC), and a humidification–dehumidification unit. Toluene was suggested as the best working fluid because the exergetic efficiency was increased by 13.26% and the unit cost of trigeneration was decreased by 6.71%.

Li et al. [13] carried out an exergy and environmental analysis of a trigeneration system coupled with rice husk gasification and solar thermal process. They found that the gasifier destroyed 39.85% of the overall exergy destruction rate. However, they estimated that the CO<sub>2</sub> emissions in the CCHP system decreased by 2.95% compared to the non-integrated system.

Zhang et al. [14] found that the exergy efficiency of a bio-gas and natural gas co-firing in a CCHP system integrated with a ground source heat pump increased by 10% when using a higher amount of natural gas. Additionally, the unit exergy cost of electricity generated by gas turbine, chilled water, and hot water decreased from 11.26 \$/GJ, 92.21 \$/GJ, and 69.92 \$/GJ to 3.84 \$/GJ, 43.52 \$/GJ, and 23.73 \$/GJ, respectively.

Ding et al. [15] conducted an exergy analysis of a cogeneration system and evaluated the effect of using different biomass feedstocks (paper, wood, paddy husks, and municipal solid waste) in the gasifier on system performance. They concluded that using municipal solid waste as the input biomass resulted in the highest exergy efficiency, 41.36%, and the lowest CO<sub>2</sub> emission, 0.9021 t/MWh. They also identified that the first and second highest exergy destruction rates were found in a combustion chamber and gas turbine.

Yang et al. [16], through the exergoeconomic analysis of a dual-fuel CCHP system based on biomass and natural gas, determined that the unit exergy cost of the products is more sensitive to the price of natural gas than to the price of biomass. In addition, they found that the exergetic efficiency increased by 5%, and the unit exergy costs of the products decreased by 2% when using only biomass.

The exergoeconomic analyses cited above have demonstrated that the operational costs and emissions can be reduced and the exergetic efficiencies increased when biofuels, instead of fossil fuels, are used in trigeneration systems. However, we have not found in the literature any study that analyzes the thermoeconomic advantages, for a particular company, of using their own waste as biofuel in a trigeneration system whose products (steam, chilled water, and power) are to be used by the plant.

In this context, this study aims to perform an exergoeconomic analysis of the system that provides steam, chilled water, and power to an instant coffee plant in Guayaquil, Ecuador. Two scenarios are considered: first, the non-integrated conventional system based on fossil fuels currently in operation at the plant, and second, a simulated CCHP system

based on a GT cycle and biofuels produced by the plant waste (SCGs). Furthermore, the impact of using different biofuels (syngas and biomass) from SCGs and fossil fuels (natural gas and fuel oil No.6) on the performance of the plant is discussed. For the analysis of the conventional system, real operational data are used.

The novelty of this paper consists of:

- The application of the exergoeconomic analysis to the heating, cooling, and power generation system of an instant coffee plant in operation.
- The evaluation of the economic and technical feasibility to replace the fossil fuels of a factory with its own agro-industrial waste.
- The analysis of the economic and exergetic effects of replacing a non-integrated system for the generation of heating, cooling, and power with a trigeneration system in the instant coffee plant in operation.

Compared with the conventional non-integrated system for generating steam, chilled water, and power, the proposed trigeneration system based on syngas and a biomass-fueled GT cycle can be more advantageous in terms of exergetic efficiency and cost of services. The findings obtained herein can be useful for re-designing similar services in agro-industrial factories with organic wastes. Additionally, this analysis can be considered a decision-making tool for choosing a fuel that increases the sustainability of the plant.

## 2. Materials and Methods

### 2.1. Conventional System Description

The conventional system of the instant coffee factory is a non-integrated system that includes a steam generator, a vapor–compression refrigeration cycle, and a diesel generator unit. A systematic diagram of the non-integrated system is presented in Figure 1. Saturated ammonia liquid enters (stream S1) the expansion valve (V-101) at 3965 kPa and leaves at 450 kPa as a liquid–vapor mixture. This mixture enters the separator (FS-101) and the liquid phase (state S3) enters the tube evaporator (HX-101), absorbs the water fluid (stream S5) heat, and exits from the evaporator as saturated steam (stream S4). The chilled water (stream S6) exits at 2 °C. The saturated steam (stream S7) is divided in to two reciprocating compressors (C-101 and C-102). The compressors have a compression ratio of 2.7 and an isentropic efficiency of 85%. The superheated steams (stream S10 and S11) enter the mixer (MX-101), and then the mixture (stream S12) enters the evaporative condenser (HX-102) and leaves as a saturated liquid.

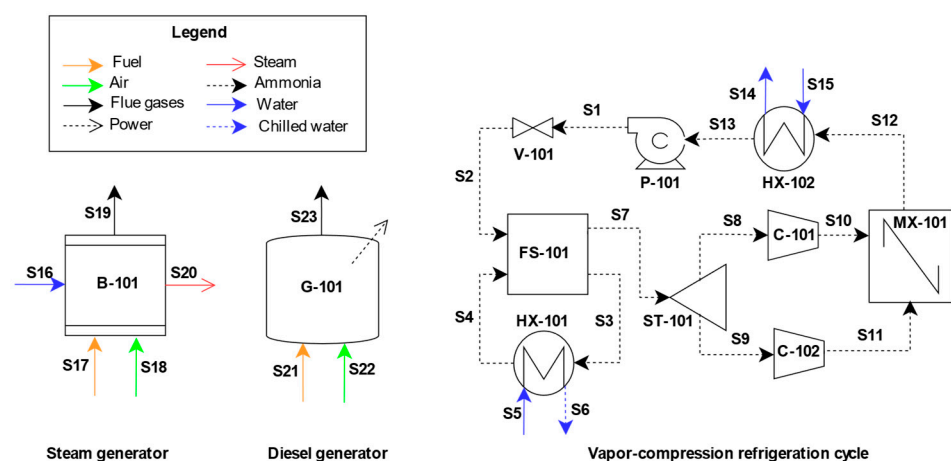


**Figure 1.** The non-integrated system of the instant coffee factory.

The diesel generator operates with an air/diesel mass ratio of 172.8 to produce 558.7 kW. The engine runs with a speed of 3000 rpm.

The steam generator is powered by fuel oil No. 6 and operates with an air/fuel mass ratio of 16 to produce 39,387 kg/h of superheated steam at 190 °C y 12,500 kPa.

## 2.2. CCHP System Description

The proposed CCHP system is based on a gas turbine (GT) cycle, a steam generator, and an absorption chiller unit. The effect of using different fuels in the proposed energy conversion system is evaluated as shown in Table 1.

**Table 1.** Four scenarios for the proposed CCHP system.

Scenario	Fuel	LHV (MJ/kg)
1	Fuel oil No.6	44.9 [17]
2	Natural gas	39.3 [18]
3	Biomass	23.4 [19]
4	Syngas	13.0 [20]

Figure 2 shows the proposed CCHP system, where power, steam, and chilled water are produced. Fuel (Stream 1) is transported by the component P-101. This component represents a pump for Scenario 1, a compressor for Scenario 2 and 4, and a screw conveyor for Scenario 3. It enters the combustion chamber (CC-101). Air (Stream 3) enters the compressor (C-101) and then enters CC-101, where complete combustion of the fuel occurs with an air/fuel mass ratio of 14.

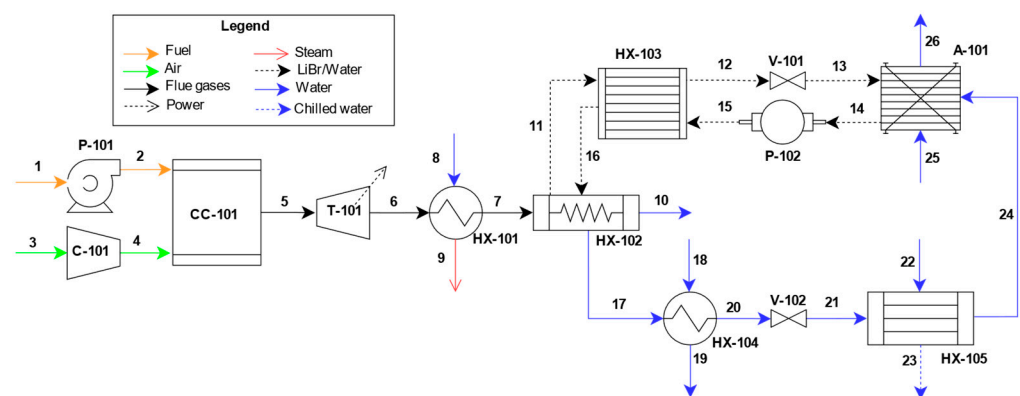


**Figure 2.** CCHP system based on biofuel from SCGs.

The flue gas (Stream 5) enters the gas turbine (T-101) with an expansion ratio of 15 and an isentropic efficiency of 70%. The turbine has a power output of 558.7 kW. Then, the flue gas (Stream 6) enters the steam generator (HX-101), where steam is generated at 190 °C and 12,500 kPa. The exhaust flue gases (Stream 7) enter the generator (HX-102), where the endothermic separation of water (Stream 11) and lithium bromide (Stream 12) occurs using the heat supplied from the flue gases. The aqueous solution of lithium bromide (Stream 14) enters the pump (P-102) with an isentropic efficiency of 85%, and then the solution enters the heat exchanger (HX-103) to absorb heat. The steam produced in the HX-102 (Stream 17) enters the condenser (HX-104). Then, the condensed water (Stream 20) enters the expansion valve (V-102) to reduce its pressure (Stream 21). Then, it enters the evaporator (HX-105). In the evaporator, the water (Stream 21) absorbs heat from a stream of water with a higher temperature (Stream 22). The stream of water that loses heat (Stream 23) leaves the evaporator as chilled water at 2 °C. The water (Stream 24) enters the absorber A-101, where it is mixed with the lithium bromide aqueous solution (Stream 13). Cooling water (Stream 25) is used in the absorber unit since the absorption process is exothermic.

## 2.3. Process Simulation

The simulation of the CCHP systems was performed in Aspen Plus V12.1. The SCGs were defined as unconventional components using the enthalpy and density models known as HCOALGEN and DCOALIGT. The proximate and ultimate analyses were specified

according to a previous study [21]. The chemical composition of natural gas [22] was obtained from the literature. The chemical composition of syngas (22.3% of hydrogen, 18.8% of carbon monoxide, 13.8% of carbon dioxide, 1.2% of methane, and 43.4% of nitrogen) was obtained from Garcia-Freites et al. [23]. Fuel oil No. 6 was defined as a pseudo component. The density and molecular weight of the fuel were obtained from the literature [24]. For the lithium bromide solution, the ELECNRTL thermodynamic model was used. For this model, it was necessary to use an electrolyte wizard to generate relevant reactions for the electrolyte solution [25].

The CC-101 combustion chamber was simulated as an adiabatic reactor using the RStoic reactor. The operational conditions of the CC-101 for each fuel were taken from previous studies: biomass [26], fuel oil No.6 [24], natural gas [27], and syngas [23]. An isentropic efficiency of 70% and an expansion ratio of 1:15 were considered for the turbine T-101 [25]. The HX-101 boiler was simulated as a shell and tube heat exchanger, and the conditions were established according to the literature for each fuel: biomass [26], fuel oil No.6 [24], natural gas [27], and syngas [23]. For the HX-101, the required heat exchange surface area was  $3.37 \text{ m}^2$  and the heat transfer coefficient was  $850 \text{ Js}^{-1}\text{m}^{-2}\text{K}^{-1}$ . The conditions of the absorber A-101, such as the temperature, pressure, and lithium bromide concentration, were taken from Somers et al. [28].

#### 2.4. Model Validation

The outlet temperature, mass flow rate, and chemical composition of the flue gases obtained in the simulated CC-101, the flue gases' outlet temperature and the thermal efficiency obtained in the simulated HX-101, and the temperature and the lithium bromide concentration in the outlet stream of the simulated A-101 were compared with the results obtained experimentally by previous studies using the same operating conditions to ensure the validity of the modeled processes.

For the system based on biomass from SCGs, the operating conditions by Prakash et al. [21] were used. For the CC-101, the air inlet temperature was  $25^\circ\text{C}$  and the air/fuel mass ratio was 12. The HX-101 had a water/fuel mass ratio of 2.5, the flue gases' inlet pressure was 8 kPa, and the flue gases' inlet temperature was  $1711^\circ\text{C}$ .

For the system based on syngas from SCGs, the operating conditions by Garcia-Freites et al. [23] were used. For the combustion chamber, the inlet air temperature was  $25^\circ\text{C}$  and the air/fuel mass ratio was 2. The HX-101 had a water/fuel mass ratio of 2.5, the flue gases' inlet pressure was 1010 kPa, and the flue gases' inlet temperature was  $1800^\circ\text{C}$ .

For the system based on fuel oil No.6, the operating conditions by Park et al. [24] were used. For the CC-101, the inlet air temperature was  $25^\circ\text{C}$  and the air/fuel mass ratio was 15. The HX-101 had a water/fuel mass ratio of 2.8:1, the flue gases' inlet pressure was 800 kPa, and the flue gases' inlet temperature was  $2118^\circ\text{C}$ .

The operating conditions by Terhan et al. [27] were used for the system based on natural gas. For the CC-101, the inlet air temperature was  $20^\circ\text{C}$  and the air/fuel mass ratio was 18. The HX-101 had a water/fuel mass ratio of 2.0, the flue gases' inlet pressure was 820 kPa, and the flue gases' inlet temperature was  $2044^\circ\text{C}$ .

The operating conditions for the absorption chiller unit were obtained from a previous experimental study [28].

#### 2.5. Exergetic Analysis

The exergetic analyses of the CCHP and the conventional systems were developed entirely using the Engineering Equation Solver (EES) V9.944 (developed by F-Chart software). The enthalpies and entropies of most of the states were calculated using the thermophysical properties of the different EES libraries. For substances that were not available in these libraries, such as SCGs, fuel oil No. 6, and diesel, the enthalpy and entropy were determined using Equations (1) and (2), respectively. The heat capacities of these substances



were taken from the literature: diesel [29], fuel oil No. 6 [30], and SCGs [31]. The dead state temperature and dead state pressure were 25 °C and 101.3 kPa, respectively.

$$\Delta H = \int_{T_{\text{ref}}}^T C_p dT \quad (1)$$

$$\Delta S = \int_{T_{\text{ref}}}^T \frac{C_p}{T} dT - \int_{P_{\text{ref}}}^P \left( \frac{\partial V}{\partial T} \right)_P dP \quad (2)$$

The physical and chemical exergy of each state was calculated using Equations (3) and (4), respectively. The standard chemical exergies were obtained using Model II [32]. In addition, the standard chemical exergies of lithium bromide [33] and ammonia [34] were taken from the literature.

$$e_i^{\text{PH}} = (h_i - h_o) - T_o(s_i - s_o) \quad (3)$$

$$e_i^{\text{CH}} = \sum x_i e_i^{\text{ch}} + R_u T_o \sum x_i \ln(x_i) \quad (4)$$

The chemical exergies of diesel and fuel oil No.6 were obtained using Equation (5) [10], valid for pure hydrocarbons.

$$e_i^{\text{CH}} = \overline{\text{HHV}} - T_o \left[ \bar{s}_{\text{fuel}} + \left( a + \frac{b}{4} \right) \bar{s}_{\text{O}_2} - a \bar{s}_{\text{CO}_2} - \frac{b}{2} \bar{s}_{\text{H}_2\text{O}} \right] + \left[ a \bar{e}_{\text{CO}_2} + \frac{b}{2} \bar{e}_{\text{H}_2\text{O}} - \left( a + \frac{b}{4} \right) \bar{e}_{\text{O}_2} \right] \quad (5)$$

where  $a$  and  $b$  represent the number of carbon atoms and hydrogen atoms in the molecule. The molecular weight of the diesel was determined using the Maxwell chart proposed by Hidalgo et al. [35]. The molecular weight of fuel oil No.6 was obtained from an estimation of an elementary analysis performed by Park et al. [24]. The  $\overline{\text{HHV}}$  of the diesel [36] and fuel oil No.6 [17] were obtained from the literature. The lower heating value for SCGs [19], syngas [20], natural gas [18], diesel [36], and fuel oil No. 6 [17] were obtained from previous studies.

The chemical exergy of dry biomass was determined using Equation (6), obtained by Song et al. [37].

$$e_{\text{SCG}}^{\text{CH}} = 1812 + 296 \cdot C + 587 \cdot H + 18 \cdot O + 18 \cdot N + 96 \cdot S - 32 \cdot A \quad (6)$$

where  $H$ ,  $C$ ,  $N$ ,  $O$ ,  $S$ , and  $A$  represent the mass fractions on a dry basis of hydrogen, carbon, oxygen, sulfur, and ash, respectively. The composition of the SCGs was determined according to the results of a previous study conducted by Vardon et al. [19].

The exergetic balance of each component presented in the process was developed according to Bejan et al. [10] using Equation (7).

$$\dot{E}_{F,k} - \dot{E}_{P,k} = \dot{E}_{D,k} - \dot{E}_{L,k} \quad (7)$$

where  $\dot{E}_{F,k}$  corresponds to the fuel exergy,  $\dot{E}_{P,k}$  is the product exergy,  $\dot{E}_{D,k}$  is the destroyed exergy, and  $\dot{E}_{L,k}$  is the exergy loss.

The exergetic efficiency for each component was determined according to Equation (8) [10].

$$\eta_{\text{ex}, k} = \left( \frac{\dot{E}_{P,k}}{\dot{E}_{F,k}} \right) \cdot 100 \quad (8)$$

Table 2 shows the definitions used to determine the fuel and product exergy rate for each component of the process.

**Table 2.** Definitions of fuel and product exergy for the system components.

Component	$\dot{E}_F$	$\dot{E}_P$
Pump (P-101)	$\dot{W}_{P-101}$	$\dot{E}_2 - \dot{E}_1$
Compressor (C-101)	$\dot{W}_{C-101}$	$\dot{E}_4 - \dot{E}_3$
Combustion chamber (CC-101)	$\dot{E}_2 + \dot{E}_4$	$\dot{E}_5$
Turbine (T-101)	$\dot{E}_5 - \dot{E}_6$	$\dot{W}_{T-101}$
Steam generator (HX-101)	$\dot{E}_6 - \dot{E}_7$	$\dot{E}_9 - \dot{E}_8$
Generator (HX-102)	$\dot{E}_7 - \dot{E}_{10}$	$(\dot{E}_{17} + \dot{E}_{11}) - \dot{E}_{16}$
Heat exchanger (HX-103)	$\dot{E}_{11} - \dot{E}_{12}$	$\dot{E}_{16} - \dot{E}_{15}$
Condenser (HX-104)	$\dot{E}_{17} - \dot{E}_{20}$	$\dot{E}_{19} - \dot{E}_{18}$
Evaporator (HX-105)	$\dot{E}_{21} - \dot{E}_{24}$	$\dot{E}_{23} - \dot{E}_{22}$
Pump (P-102)	$\dot{W}_{P-102}$	$\dot{E}_{15} - \dot{E}_{14}$
Absorber (A-101)	$(\dot{E}_{26} - \dot{E}_{25}) + \dot{E}_{24}$	$\dot{E}_{13} - \dot{E}_{14}$

## 2.6. Economic Analysis

The economic analysis of the proposed system was carried out following the revenue requirement method for thermal systems offered by Bejan et al. [10]. The purchase equipment costs (PEC) were determined based on the specific characteristics of each component in the system. The chemical engineering plant cost index (CEPCI) of 607.5 was used in this study to adjust the PEC of each component for 2019.

Equation (9) [34] was used to calculate the PEC in the case of the evaporators, pumps, and heat exchangers.

$$PEC = a + b \cdot S^n \quad (9)$$

where  $a$ ,  $b$ , and  $n$  are the cost constants and  $S$  is the size parameter of each component. Table 3 shows the values of the constants and parameters for each component for the year 2010; the CEPCI for this year was 532.9 [38].

**Table 3.** Cost constants and size parameters.

Components	A	b	n	S
Evaporators	330	36,000	0.55	0.36 (m <sup>2</sup> )
Pumps	8000	240	0.9	2.22 (L/s)
Heat exchangers	28,000	54	1.2	3.15 (m <sup>2</sup> )

The equations used for the determination of the PEC of the turbine [39], the compressor [10], the combustion chamber [40], and the condenser [41] are presented in Table 4.

**Table 4.** Mathematical equations for the purchase equipment costs.

PEC Equation	Year	CEPCI	Equation No.
$\log_{10}(PEC_{T-101}) = 2.2476 + 1.4965 \cdot \log_{10}(A_i) - 0.1618 \cdot [\log_{10}(A_i)]^2$	2001	397	(10)
$PEC_{C-101} = \left( \frac{71.1 \cdot \dot{m}}{0.9 - \eta_{isen,eff}} \right) \left( \frac{P_{out}}{P_{in}} \right) \ln \left( \frac{P_{out}}{P_{in}} \right)$	1982	315	(11)
$PEC_{CC-101} = \frac{28.98 \cdot \dot{m}_{air}}{0.995 \left( \frac{P_{out}}{P_{in}} \right)} \cdot \left( 1 + e^{(0.015(T_{out} - 1540))} \right)$	2003	402	(12)
$PEC_{HX-104} = 281 \cdot \frac{\dot{Q}_{HX-104}}{2200 \left[ \frac{(T_{in,hs} - T_{out,cs}) - (T_{out,hs} - T_{in,cs})}{\ln \left( \frac{T_{in,hs} - T_{out,cs}}{T_{out,hs} - T_{in,cs}} \right)} \right]} + 746 \cdot \dot{m}_{out}$	1982	315	(13)

The natural gas and diesel costs were \$0.0894/kg [18] and \$0.6381/kg [42]. The cost of water and power electricity in Guayaquil, Ecuador, were \$0.72/m<sup>3</sup> [43] and \$0.0756/kWh [44]. The cost of syngas and the biomass from SCGs were obtained from a previous study by

the authors [45]. The fuel oil No. 6, lithium bromide, and ammonia costs were \$0.257/kg, \$0.30/kg, and \$0.60/kg, respectively, which were obtained directly from different suppliers.

The total operating and maintenance cost rate was determined for each component present in the system using Equation (14) [10].

$$\dot{Z}_k = \dot{Z}_k^{\text{O\&M}} + \dot{Z}_k^{\text{CI}} \quad (14)$$

where  $\dot{Z}_k^{\text{CI}}$  refers to the cost rate associated with the capital investment and  $\dot{Z}_k^{\text{O\&M}}$  refers to the cost rate for operation and maintenance. The economic indicators used to calculate the total operating and maintenance cost rates [10] are specified in Table 5.

**Table 5.** Economic parameters for the economic analysis.

Component	Fuel Cost
Average general inflation rate	0.05
Average nominal escalation rate of all costs	0.05
Average nominal escalation rate of fuel costs	0.06
Plant economic life in years (n)	20
Plant life for tax purposes in years	15
Combined average income tax rate	0.38
Average property tax rate (%PFI)	0.015
Average insurance rate (%PFI)	0.5
Average capacity factor	0.85
Labor positions for O&M	20
Average labor cost (\$/h)	18

## 2.7. Exergoeconomic Analysis

The exergoeconomic analysis was performed for each of the components of the system using Equation (15) [10]:

$$\dot{C}_{F,k} + \dot{Z}_k = \dot{C}_{P,k} \quad (15)$$

where  $\dot{C}_{F,k}$  and  $\dot{C}_{P,k}$  represent the fuel and product cost rates, respectively. The exergy destroyed in the k-th component has an associated cost rate  $\dot{C}_{D,k}$  that can be calculated in terms of the cost of the additional fuel ( $c_{F,k}$ ) that needs to be supplied to this component to cover the exergy destruction and to generate the same exergy flow rate of the product, when  $\dot{E}_{P,k}$  stay constant (Equation (16)).

$$\dot{C}_{D,k} = c_{F,k} \dot{E}_{D,k} \quad (16)$$

The fuel and product cost equations and the auxiliary equations for the proposed system are presented in Table 6.

**Table 6.** Cost balance equations and auxiliary equations for exergy costs of the system.

Component	Fuel Cost	Product Cost	Auxiliary Equations
Pump (P-101)	$\dot{W}_{P-101} \cdot c_{ep}$	$\dot{C}_2 - \dot{C}_1$	-
Compressor (C-101)	$\dot{W}_{C-101} \cdot c_{ep}$	$\dot{C}_4 - \dot{C}_3$	-
Combustion chamber (CC-101)	$\dot{C}_2 + \dot{C}_4$	$\dot{C}_5$	-
Turbine (T-101)	$\dot{C}_5 - \dot{C}_6$	$\dot{W}_{T-101} \cdot c_{ep}$	-
Steam generator (HX-101)	$\dot{C}_6 - \dot{C}_7$	$\dot{C}_9 - \dot{C}_8$	$c_6 = c_7$
Generator (HX-102)	$\dot{C}_7 - \dot{C}_{10}$	$(\dot{C}_{17} + \dot{C}_{11}) - \dot{C}_{16}$	$c_7 = c_{10}$
Heat exchanger (HX-103)	$\dot{C}_{11} - \dot{C}_{12}$	$\dot{C}_{16} - \dot{C}_{15}$	$c_{11} = c_{12}$
Condenser (HX-104)	$\dot{C}_{17} - \dot{C}_{20}$	$\dot{C}_{19} - \dot{C}_{18}$	$c_{18} = c_{19}$
Evaporator (HX-105)	$\dot{C}_{21} - \dot{C}_{24}$	$\dot{C}_{23} - \dot{C}_{22}$	$c_{21} = c_{24}$
Pump (P-102)	$\dot{W}_{P-102} \cdot c_{ep}$	$\dot{C}_{15} - \dot{C}_{14}$	-
Absorber (A-101)	$(\dot{C}_{26} - \dot{C}_{25}) + \dot{C}_{24}$	$\dot{C}_{13} - \dot{C}_{14}$	$c_{25} = c_{26}$



### 3. Results and Discussion

#### 3.1. Model Validation

The values of the main operating parameters obtained in this work have been compared with those reported in experimental studies from other literature to verify the validity of the proposed model for each scenario. In Table 7, the outlet temperature, the CO<sub>2</sub> and O<sub>2</sub> concentration of flue gases of the combustion chamber (CC-101), the outlet mass flow rate and temperature of flue gases, the thermal efficiency of the steam generator (HX-101), and the outlet temperature and LiBr concentration of the absorber are presented and compared.

**Table 7.** Results of model validation.

Fuel	Component	Parameter	This Work	Literature	Relative Error (%)
Natural Gas	CC-101	Outlet temperature of flue gases (°C)	2252	2248 [27]	0.18
		CO <sub>2</sub> (%mol)	8.7	8.5 [27]	2.35
		Mass flow rate of flue gases (kg/s)	1.85	1.90 [27]	2.63
	HX-101	Outlet temperature of flue gases (°C)	774.7	770 [27]	0.61
		Thermal efficiency (%)	89.0	94	5.3
Fuel oil No.6	CC-101	Outlet temperature of flue gases (°C)	2338	2340 [24]	0.08
		CO <sub>2</sub> (%mol)	13	12 [24]	8.30
		Mass flow rate of flue gases (kg/s)	1.82	2.01 [24]	9.45
	HX-101	Outlet temperature of flue gases (°C)	775.7	780 [24]	0.55
		Thermal efficiency (%)	81.8	93	12.0
Syngas	CC-101	Outlet temperature of flue gases (°C)	1987	1985 [23]	0.10
		CO <sub>2</sub> (%mol)	16.4	13 [23]	20.7
		Mass flow rate of flue gases (kg/s)	2.11	1.47 [23]	30.3
	HX-101	Outlet temperature of flue gases (°C)	645	649.5 [23]	0.69
		Thermal efficiency (%)	94.4	95	0.6
Biomass	CC-101	Outlet temperature of flue gases (°C)	1908	1910 [21]	0.10
		CO <sub>2</sub> (%mol)	9.2	10.5 [21]	12.4
		Mass flow rate of flue gases (kg/s)	2.17	1.5 [21]	30.8
	HX-101	Outlet temperature of flue gases (°C)	508.6	512 [21]	0.66
		Thermal efficiency (%)	91.1	95	4.1
-	A-101	Outlet temperature (°C)	32.7	32.7 [28]	0
		Outlet LiBr concentration (%)	0.574	0.574 [28]	0

It can be seen that the results of the model for each fuel are close to the results reported in the experimental studies. Hence, the model can be used successfully to describe the CCHP system applying different fuels such as natural gas, fuel oil No.6, syngas, and biomass under established operational conditions.

#### 3.2. Exergetic Analysis

The exergetic analysis was performed on the conventional system based on fuel oil No.6 (base case) and the CCHP systems based on different fuels. The overall exergy destruction rate of each case is presented in Figure 3a. It can be seen that the CCHP system based on fuel oil No.6 shows a lower exergy destruction rate than the base case based on the same fuel. Furthermore, the CCHP based on syngas has the lowest exergy destruction rate. The CCHP system based on biomass from SCGs also has a low exergy destruction rate compared with the same system based on natural gas. Similar results were obtained by Gholizadeh et al. [12], who concluded that using biomass (from crop straw) reduced the exergy destruction rate of a CCHP system.

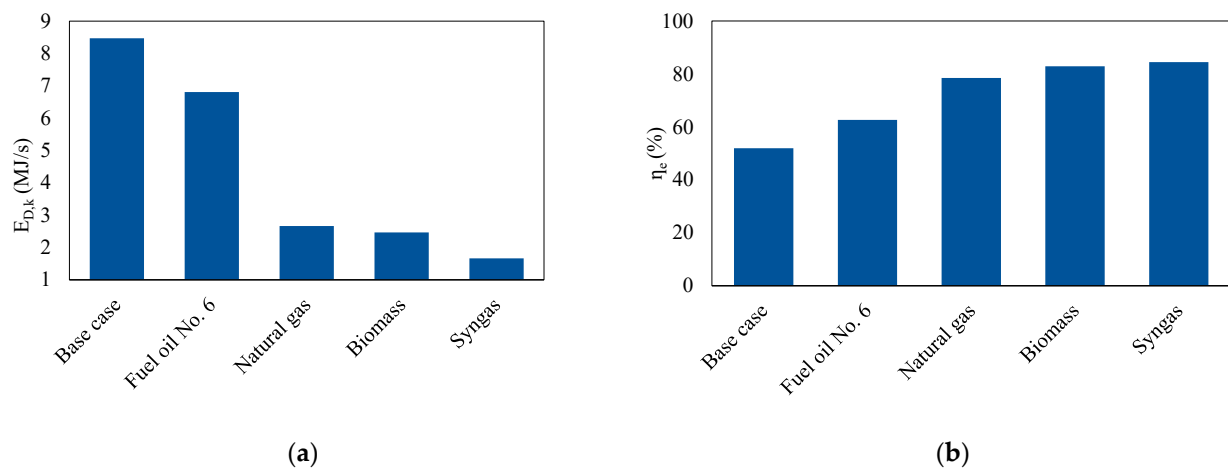


**Figure 3.** Comparisons of (a) the exergy destruction rate and (b) the exergy efficiency of the base case and the CCHP using different fuels.

Figure 3b shows the overall exergetic efficiency of the conventional system (base case) and CCHP systems based on different fuels. It is observed that the CCHP systems based on syngas and biomass have the highest exergetic efficiency (84.4% and 82.9%, respectively). The base case and the CCHP systems based on fossil fuels have the lowest exergetic efficiency (51.9%). Similar findings were found by Yang et al. [16], who concluded that a mixture of fuel (sugarcane bagasse and natural gas) increased the exergetic efficiency by 4.1% and that the exergy costs decreased by 2%.

Figure 4a shows the exergy destruction rate for the eight components, with the highest exergy destruction rate seen in the CCHP system based on different fuels. It can be seen that the combustion chambers based on syngas and biomass have a lower exergy destruction rate than the combustion chamber based on fuel oil No.6. In addition, the exergy destruction rate of the combustion chamber (CC-101) from the CCHP system based on fuel oil No.6 represents 62.7% of the overall exergy destruction rate. The low exergetic efficiency of the combustion chamber based on fuel oil No.6 is due, mostly, to the high concentration of impurities in this fuel oil. Similar results were obtained by Miar et al. [46] when analyzing a CCHP system based on natural gas. Additionally, Marques et al. [47] determined that the combustion engine in the CCHP system based on natural gas was the component with the highest irreversibilities, around 87.8% of the overall system.

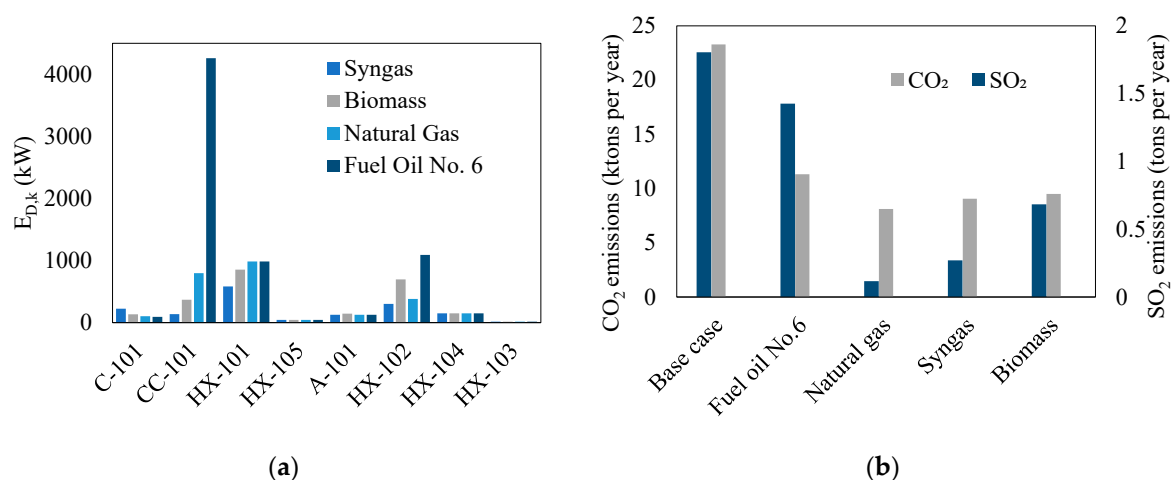


**Figure 4.** Comparison of (a) exergy destruction rate at a level component and (b) CO<sub>2</sub> and SO<sub>2</sub> emissions from the CCHP system based on different fuels.

It is observed that the components HX-101 (boiler) and HX-102 (generator) employing fuel oil No.6 also have high exergy destruction rates than other components of the system; 985 kW and 1090 kW, respectively. Similar findings were obtained by Miar et al. [48], who concluded that the exergy destruction rate of the boiler represented 61.57% of the overall CHP system based on sugarcane bagasse (biomass). Furthermore, the components with the lowest exergy destruction rate were the turbine T-101 and the pumps.

Furthermore, the CO<sub>2</sub> and SO<sub>2</sub> emissions are reported in Figure 4b. The results were obtained from the simulation of the combustion process. It is observed that the base case has the highest CO<sub>2</sub> and SO<sub>2</sub> emissions, while the systems based on biofuels have reduced CO<sub>2</sub> emissions by 61.1% and SO<sub>2</sub> emissions by 85%. These findings are in line with previous studies where high values of greenhouse gas emissions were observed when using fossil fuels in a CCHP system [49].

### 3.3. Exergoeconomic Analysis

The exergoeconomic analysis was performed on the conventional system based on fuel oil No.6 (base case) and the CCHP systems based on different fuels. Figure 5a shows the total investment cost for each plant. The initial investment cost for the plant was 5.17 million dollars, while for the proposed CCHP systems, the costs are between 2.34 and 2.49 million dollars. The most expensive components of the plant are the compressor of the conventional refrigeration system, the diesel generator, and the steam generator. The initial investment cost for the systems based on biofuels is 6% less than the investment cost for the proposed system based on Fuel No.6.

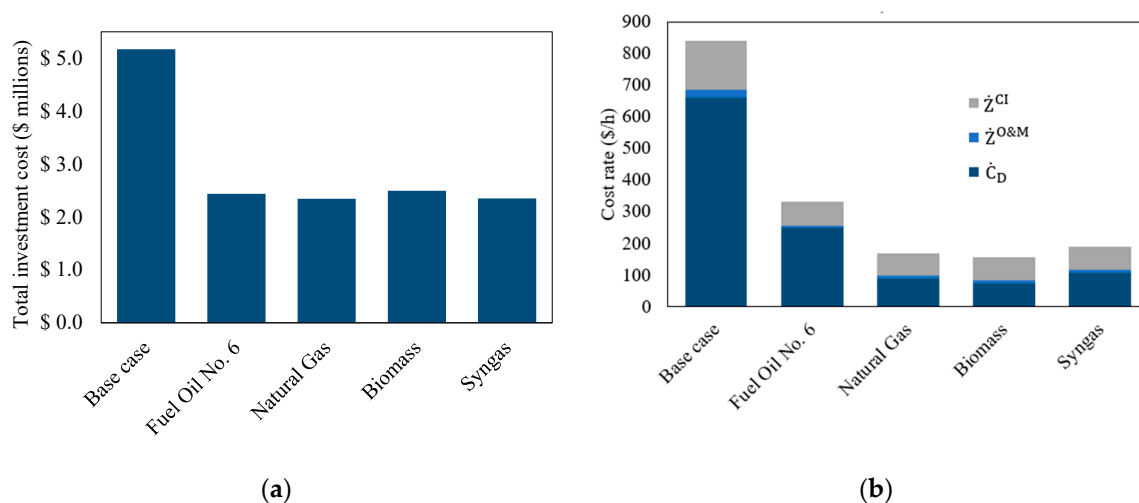


**Figure 5.** Comparison of (a) Total investment cost of the plant and (b) Exergy destruction, investment, and O&M cost rates of the CCHP system based on different fuels.

Figure 5b shows the relation between the overall exergy destruction cost rates and the capital investment and O&M cost rates for each system based on different fuels. In general terms, the exergy destruction cost rate represents between 48.5% and 78.5% of the overall cost. The irreversibilities in the biomass-based CCHP system have a low impact on the overall cost rate; however, the destroyed exergy in the base case has the highest impact on the operational cost rate. In addition, it is observed that the investment and O&M cost rate is higher in the conventional system than in the CCHP systems. The compressor, the diesel generator, and the steam generator of the conventional system are responsible for 92.6% of the overall investment and O&M cost rate. However, using fossil fuels in the CCHP system has not significantly reduced the cost rates of the systems based on biofuels.

Figure 6 shows the distribution of the exergy destruction cost rate ( $\dot{C}_{D,k}$ ) at a level component for the CCHP system based on different fuels and the base case. It can be seen in the system based on fuel oil No. 6 that the components with the highest total operational

cost rates, in decreasing order, are combustion chamber CC-101 (21.6%), condenser HX-104 (17.2%), generator HX-102 (16.8%), and steam generator HX-101 (15.5%), while for the system based on syngas, these components have low exergy destruction cost rates. Similarly, Marques et al. [47] determined in a CCHP system based on natural gas that the component with the highest cost rates was the internal combustion engine (63.7%), followed by the steam generator (19.8%). Additionally, Wang et al. [50] found that the combustion chamber and the steam generator were the components with the highest exergy destruction cost rate in a trigeneration system based on biomass from wood.

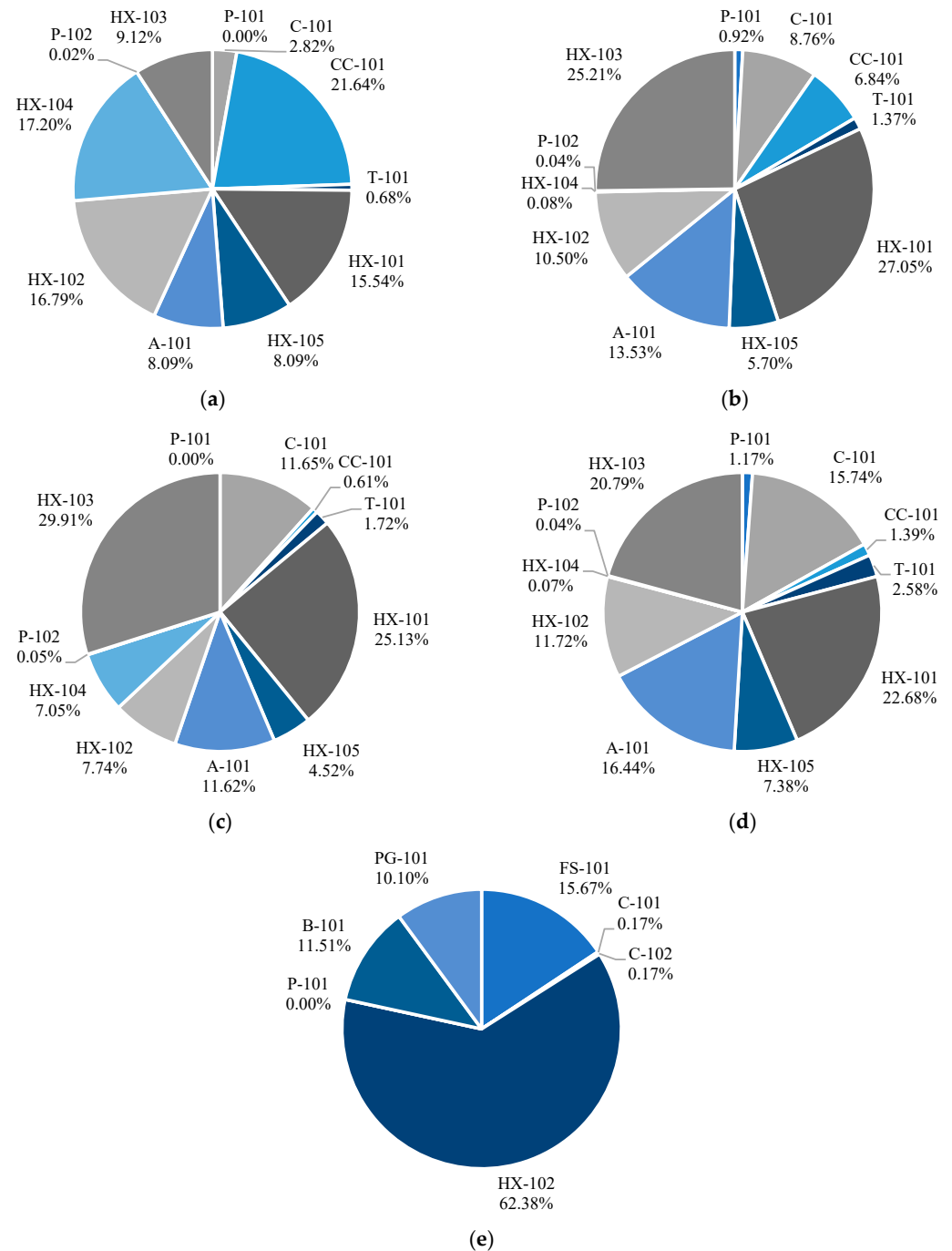


**Figure 6.** Exergy destruction cost rate of the CCHP system at a component level based on: (a) Fuel oil No. 6, (b) Natural gas, (c) Biomass, (d) Syngas, and (e) Base case.

For the conventional system, the scenario is different. The component with the highest exergy destruction cost rate is the condenser HX-102 of the vapor compression refrigeration cycle, followed by the evaporator HX-101 that produced the chilled water for the factory. The steam generator B-101 is the third component with the highest exergy destruction cost rate. These results show that a non-integrated system increases the cost of facilities for the plant.

Table 8 shows the cost of the steam, chilled water, and power for each CCHP system based on different fuels and the conventional system obtained from the exergoeconomic analysis. The conventional and CCHP systems based on fuel oil No.6 have the highest cost for most services. It is observed that when natural gas is used instead of syngas, the cost of the services is reduced. This occurs because the specific cost of natural gas is lower than the cost of syngas. In addition, the LHV of syngas is lower than that of natural gas.

**Table 8.** Comparison of the exergy costs for the base case and CCHP systems with different fuels.

Fuel	Steam Cost (\$/GJ)	Chilled Water Cost (\$/GJ)	Power Cost (\$/GJ)
Base case	24.60	30.20	89.92
Fuel oil No.6	17.97	40.35	29.41
Natural gas	11.75	22.30	24.40
Syngas	16.49	25.77	30.07
Biomass	10.26	20.22	23.43

However, it is shown that the use of biomass allows for reducing steam costs by 58.3%, chilled water by 33.1%, and power costs by 73.9%. These results are consistent with the previous literature. For example, Ghaebi et al. [51] analyzed a CCHP system based on liquified natural gas, finding that the cost of power, heating output, and cooling output were 45.62 \$/GJ, 193.3 \$/GJ, and 62.88 \$/GJ, respectively. In addition, Wu et al. [11] determined that when using straw as biomass in a CCHP system, the power, heating, and cooling outputs were 45.55 \$/GJ, 185.0 \$/GJ, and 236.6 \$/GJ, respectively. The costs when using straw as biomass are higher than reported in this study because straw had a higher specific cost (0.051 \$/kg). This shows the importance of having organic waste as a source of biomass, since the cost is considerably reduced.

#### 4. Conclusions

A trigeneration system for heating, power, and cooling production was devised based on a biofuel-fueled GT cycle and absorption chiller unit. The system was simulated using different fuels such as syngas and biomass from SCGs, natural gas, and fuel oil No.6. All the models were validated with experimental data, achieving a maximum relative error of 9.45%. In addition, the feasibility of the systems was investigated from exergy and economic viewpoints. The main conclusions obtained from this study are presented below:

- The overall exergetic efficiency of the conventional system is 51.9% and the total exergy destruction rate is 8.5 MJ/s. Over 59.2% of the total exergy destruction rate in the conventional system occurs in the steam generator. The CCHP systems increased exergetic efficiency between 62.6% and 84.5%, and reduced the exergy destruction rate between 1.66 MJ/s and 6.81 MJ/s.
- The exergy destruction cost rate of the conventional system (\$660.8/h) represents 78.5% of the total cost rate of the plant. Among all components, the condenser has the highest exergy destruction cost rate (\$412.2 /h). By contrast, the CCHP system based on biomass obtained the lowest overall exergy destruction cost rate (\$75.4/h).
- Furthermore, the CO<sub>2</sub> and SO<sub>2</sub> emissions of the conventional system are 23,283 and 1.8 tons per year, respectively. However, the CCHP reduced the CO<sub>2</sub> and SO<sub>2</sub> emissions by 65.1% and 93.5%, respectively.
- Compared with the conventional non-integrated system for the generation of steam, chilled water, and power, the results show that the proposed trigeneration system

based on syngas and biomass-fueled GT cycle is more advantageous in terms of the exergy efficiency, the CO<sub>2</sub> and SO<sub>2</sub> emissions, and the cost of services.

- In addition, out of the four fuels screened through the trigeneration systems, biomass is considered economically feasible due to its lower investment and operating costs (\$2.49 million and \$8.04/h, respectively).
- Using biomass as fuel instead of syngas in the trigeneration system reduces the steam, chilled water, and power costs by around 37.8%, 21.5%, and 22.1%, respectively.

This study demonstrates that is economically and technically feasible to operate a CCHP system instead of a non-integrated system in a factory for heating, power, and cooling production. The reduction in greenhouse gas emissions is also a benefit for the industrial sector because it could reduce their carbon footprint. Furthermore, the use of biofuels such as syngas or biomass from agro-industrial waste contributes to reducing the environmental impact of the industrial processes.

In order to optimize the proposed systems, future research should focus on the analysis of dual systems to integrate different sources of energy. Furthermore, an advanced exergoeconomic analysis should be performed to quantify the avoidable exergy destruction cost rate, mainly in the steam generator and the condenser. In addition, experimental research at a pilot scale would be recommendable to develop an extended validation of the proposed model of the CCHP system based on biomass from SCGs.

**Author Contributions:** Conceptualization, D.L.T.C.; methodology, A.M.B.M.; software, O.P.L., M.S.T. and M.M.-B.; validation, O.P.L. and M.S.T.; investigation, D.L.T.C.; formal analysis, D.L.T.C.; data curation, O.P.L. and M.S.T.; writing—original draft preparation, M.M.-B. and D.L.T.C.; writing—review and editing, A.M.B.M.; supervision, A.M.B.M. and A.L.M.; project administration, A.M.B.M. and A.L.M. All authors have read and agreed to the published version of the manuscript.

**Funding:** This research received no external funding.

**Data Availability Statement:** No new data were created or analyzed in this study. Data sharing is not applicable to this article.

**Conflicts of Interest:** The authors declare no conflict of interest.

## Nomenclature

Symbol	
A	ash mass fraction on a dry basis
C	carbon mass fraction on a dry basis
$\dot{C}$	the cost associated with an exergy stream (\$/h)
C <sub>p</sub>	specific heat at constant pressure (kJ/kg-K)
c	unit exergy cost (\$/kJ)
$\dot{E}$	exergy rate (kW)
e	specific exergy rate (kJ/kg)
HHV	higher heating value (mol/kJ)
H	hydrogen mass fraction on a dry basis
h	specific enthalpy (kJ/kg)
$\dot{m}$	mass flowrate (kg/s)
N	nitrogen mass fraction on a dry basis
n	lifetime of the system (years)
O	oxygen mass fraction on a dry basis
P	pressure (kPa)
$\dot{Q}$	rate of heat (W)
R	ideal gas constant (kJ/kmol-K)
S	sulfur mass fraction on a dry basis
s	specific entropy (kJ/kg-K)
T	temperature (K)
v	stoichiometric coefficient
$\dot{W}$	power (kW)



x	mole fraction
$\dot{Z}$	investment cost rate (\$/h)
Greek letters	
$\eta$	exergetic efficiency (%)
$\Delta$	difference
Superscript	
CI	investment cost
CH	chemical
O&M	operation and maintenance
PH	physical
Subscript	
cs	cold stream
D	destroyed
EP	electric power
F	fuel
hs	hot stream
i	ith compound
k	kth component
L	loss
P	product
Abbreviations	
A	absorber
CCHP	combined cooling, heating, and power
CC	combustion chamber
C	compressor
ELECNRTL	electrolyte NRTL
FS	flash separator
GT	gas turbine
HX	heat exchanger
GN	natural gas
MX	mixer
O&M	operation and maintenance
PFI	plant–facilities investment
P	pump
PEC	purchase equipment cost
SCGs	spent coffee grounds
ST	splitter
SG	syngas
T	turbine
V	valve

## References

- Jiang, J.; Gao, W.; Gao, Y.; Wei, X.; Kuroki, S. Performance Analysis of CCHP System for University Campus in North China. *Procedia-Soc. Behav. Sci.* **2016**, *216*, 361–372. [\[CrossRef\]](#)
- Prakash, M.; Sarkar, A.; Sarkar, J.; Chakraborty, J.P.; Mondal, S.S.; Sahoo, R.R. Performance assessment of novel biomass gasification based CCHP systems integrated with syngas production. *Energy* **2019**, *167*, 379–390. [\[CrossRef\]](#)
- Correa, C.; Alves, Y.A.; Souza, C.G.; Boloy, R.A.M. Brazil and the world market in the development of technologies for the production of second-generation ethanol. *Alex. Eng. J.* **2022**, *67*, 153–170. [\[CrossRef\]](#)
- Jaroenhasemmesuk, C.; Tipayawong, N.; Shimpalee, S.; Ingham, D.B.; Pourkashanian, M. Improved simulation of lignocellulosic biomass pyrolysis plant using chemical kinetics in Aspen Plus® and comparison with experiments. *Alex. Eng. J.* **2022**, *63*, 199–209. [\[CrossRef\]](#)
- Sadi, M.; mohammad Behzadi, A.; Alsagri, A.S.; Chakravarty, K.H.; Arabkoohsar, A. An innovative green multi-generation system centering around concentrating PVTs and biomass heaters, design and multi-objective optimization. *J. Clean. Prod.* **2022**, *340*, 130625. [\[CrossRef\]](#)
- Sadi, M.; Chakravarty, K.; Behzadi, A.; Arabkoohsar, A. Techno-economic-environmental investigation of various biomass types and innovative biomass-firing technologies for cost-effective cooling in India. *Energy* **2021**, *219*, 119561. [\[CrossRef\]](#)
- Abdel Daiem, M.M.; Said, N. Energetic, economic, and environmental perspectives of power generation from residual biomass in Saudi Arabia. *Alex. Eng. J.* **2022**, *61*, 3351–3364. [\[CrossRef\]](#)

8. Giuliano, A.; Catizzzone, E.; Freda, C. Process simulation and environmental aspects of dimethyl ether production from digestate-derived syngas. *Int. J. Environ. Res. Public Health* **2021**, *18*, 807. [CrossRef] [PubMed]
9. Sofia, D.; Giuliano, A.; Barletta, D. Techno-economic assessment of co-gasification of coal-petcoke and biomass in IGCC power plants. *Chem. Eng. Trans.* **2013**, *32*, 1231–1236.
10. Bejan, A.; Tsatsaronis, G.; Moran, M. *Thermal Design & Optimization*; John Wiley & Sons, Inc.: Toronto, ON, Canada, 1996; ISBN 0-471-58467-3.
11. Wu, J.; Wang, J.; Wu, J.; Ma, C. Exergy and exergoeconomic analysis of a combined cooling, heating, and power system based on solar thermal biomass gasification. *Energies* **2019**, *12*, 2418. [CrossRef]
12. Gholizadeh, T.; Vajdi, M.; Rostamzadeh, H. Exergoeconomic optimization of a new trigeneration system driven by biogas for power, cooling, and freshwater production. *Energy Convers. Manag.* **2020**, *205*, 112417. [CrossRef]
13. Li, H.; Zhang, X.; Liu, L.; Zeng, R.; Zhang, G. Exergy and environmental assessments of a novel trigeneration system taking biomass and solar energy as co-feeds. *Appl. Therm. Eng.* **2016**, *104*, 697–706. [CrossRef]
14. Zhang, X.; Zeng, R.; Mu, K.; Liu, X.; Sun, X.; Li, H. Exergetic and exergoeconomic evaluation of co-firing biomass gas with natural gas in CCHP system integrated with ground source heat pump. *Energy Convers. Manag.* **2019**, *180*, 622–640. [CrossRef]
15. Ding, H.; Li, J.; Heydarian, D. Energy, exergy, exergoeconomic, and environmental analysis of a new biomass-driven cogeneration system. *Sustain. Energy Technol. Assess.* **2021**, *45*, 101044. [CrossRef]
16. Yang, K.; Zhu, N.; Ding, Y.; Chang, C.; Wang, D.; Yuan, T. Exergy and exergoeconomic analyses of a combined cooling, heating, and power (CCHP) system based on dual-fuel of biomass and natural gas. *J. Clean. Prod.* **2019**, *206*, 893–906. [CrossRef]
17. Government of Canada. Stack Losses for Heavy No. 6 Fuel Oil. Available online: <https://www.nrcan.gc.ca/mining-materials/publications/boiler-system-energy-losses/stack-losses-general-methodology/stack-losses-heavy-no-6-fuel-oil/5443> (accessed on 5 May 2022).
18. Eswara, A.K.; Misra, S.C.; Ramesh, U.S. Introduction to natural gas: A comparative study of its storage, fuel costs and emissions for a harbor tug. In Proceedings of the Annual Meeting of Society of Naval Architects & Marine Engineers (SNAME), Bellevue, WA, USA, 8 November 2013; pp. 1–21.
19. Vardon, D.R.; Moser, B.R.; Zheng, W.; Witkin, K.; Evangelista, R.L.; Strathmann, T.J.; Rajagopalan, K.; Sharma, B.K. Complete utilization of spent coffee grounds to produce biodiesel, bio-oil, and biochar. *ACS Sustain. Chem. Eng.* **2013**, *1*, 1286–1294. [CrossRef]
20. Kibret, H.A.; Kuo, Y.L.; Ke, T.Y.; Tseng, Y.H. Gasification of spent coffee grounds in a semi-fluidized bed reactor using steam and CO<sub>2</sub> gasification medium. *J. Taiwan Inst. Chem. Eng.* **2021**, *119*, 115–127. [CrossRef]
21. Prakash, M.; Sarkar, A.; Sarkar, J.; Mondal, S.S.; Chakraborty, J.P. Proposal and design of a new biomass based syngas production system integrated with combined heat and power generation. *Energy* **2017**, *133*, 986–997. [CrossRef]
22. Chan, S.H.; Wang, H.M. Effect of natural gas composition on autothermal fuel reforming products. *Fuel Process. Technol.* **2000**, *64*, 221–239. [CrossRef]
23. Garcia-Freites, S.; Welfle, A.; Lea-Langton, A.; Gilbert, P.; Thornley, P. The potential of coffee stems gasification to provide bioenergy for coffee farms: A case study in the Colombian coffee sector. *Biomass Convers. Biorefinery* **2020**, *10*, 1137–1152. [CrossRef]
24. Park, H.Y.; Han, K.; Kim, H.H.; Park, S.; Jang, J.; Yu, G.S.; Ko, J.H. Comparisons of combustion characteristics between bioliquid and heavy fuel oil combustion in a 0.7 MWth pilot furnace and a 75 MWe utility boiler. *Energy* **2020**, *192*, 116557. [CrossRef]
25. Hajabdollahi, Z.; Fu, P.F. Multi-objective based configuration optimization of SOFC-GT cogeneration plant. *Appl. Therm. Eng.* **2017**, *112*, 549–559. [CrossRef]
26. Kang, S.B.; Oh, H.Y.; Kim, J.J.; Choi, K.S. Characteristics of spent coffee ground as a fuel and combustion test in a small boiler (6.5 kW). *Renew. Energy* **2017**, *113*, 1208–1214. [CrossRef]
27. Terhan, M.; Comakli, K. Energy and exergy analyses of natural gas-fired boilers in a district heating system. *Appl. Therm. Eng.* **2017**, *121*, 380–387. [CrossRef]
28. Somers, C.; Mortazavi, A.; Hwang, Y.; Radermacher, R.; Rodgers, P.; Al-Hashimi, S. Modeling water/lithium bromide absorption chillers in ASPEN Plus. *Appl. Energy* **2011**, *88*, 4197–4205. [CrossRef]
29. Odebumni, E.O.; Ogunsakin, E.A.; Ilukor, P.E.P. Characterization of crude oil and petroleum products. *Bull. Chem. Soci. Ethiop.* **2002**, *16*, 115–132.
30. Cragoe, C.S. *Thermal Properties of Petroleum Products: November 9, 1929*—Carl Susan Cragoe—Google Libros; US Government Printing Office: Washington, DC, USA, 1929.
31. Afolabi, O.O.D.; Sohail, M.; Cheng, Y.L. Optimisation and characterisation of hydrochar production from spent coffee grounds by hydrothermal carbonisation. *Renew. Energy* **2020**, *147*, 1380–1391. [CrossRef]
32. Szargut, J.; Morris, D.R.; Steward, F.R. *Exergy Analysis of Thermal, Chemical, and Metallurgical Processes*; Hemisphere Publishing Corporation: New York, NY, USA, 1987.
33. Baratto, J.; Gallego, J. Análisis Exergético De Un Sistema De Refrigeración Por Absorción De Doble Efecto Con Eyecto-Compresión. *Repos. Univ. Tecnol. Pereira* **2014**, *53*, 123.
34. Bakshi, B.R.; Gutowski, T.; Sekulić, D.P. (Eds.) *Thermodynamics and the Destruction of Resources*—Google Libros; Cambridge University Press: Cambridge, UK, 2011.

35. Hidalgo, E. Estimación de emisiones gaseosas de Fuentes fijas en el sector industrial del Cantón Rumiñahui. Bachelor's Thesis, Universidad Central del Ecuador, Quito, Ecuador, 2014.
36. Staffell, I. *The Energy and Fuel Data Sheet*; University of Birmingham: Birmingham, UK, 2011.
37. Song, G.; Shen, L.; Xiao, J. Estimating specific chemical exergy of biomass from basic analysis data. *Ind. Eng. Chem. Res.* **2011**, *50*, 9758–9766. [[CrossRef](#)]
38. Towler, G.; Sinnott, R. *Chemical Engineering Design-Principles, Practice and Economics of Plant and Process Design*, 2nd ed.; Elsevier Inc.: Amsterdam, The Netherlands, 2012.
39. Kolahi, M.; Yari, M.; Mahmoudi, S.M.S.; Mohammadkhani, F. Thermodynamic and economic performance improvement of ORCs through using zeotropic mixtures: Case of waste heat recovery in an offshore platform. *Case Stud. Therm. Eng.* **2016**, *8*, 51–70. [[CrossRef](#)]
40. Amidpour, M.; Man, M.H.K. *Cogeneration and Polygeneration Systems*, 1st ed.; Academic Press: Cambridge, MA, USA, 2020.
41. Abam, F.I.; Briggs, T.A.; Ekwe, E.B.; Effiom, S.O. Investigation of intercooler-effectiveness on exergo-economic and exergo-sustainability parameters of modified Brayton cycles. *Case Stud. Therm. Eng.* **2017**, *10*, 9–18. [[CrossRef](#)]
42. PetroEcuador, E.P. *Precios de Venta a Nivel de Terminal Para las Comercializadoras Calificadas y Autorizadas a Nivel Nacional*; Petroecuador EP: Quito, Ecuador, 2016.
43. International Water Services Interagua, C. *Ltda. Informe Anual 2018–2019*; Interagua: Guayaquil, Ecuador, 2019.
44. Macías Centeno, J.E.; Valarezo Molina, L.A.; Llor Castillo, G. Los Diferentes Costos que Tiene la Energía Eléctrica en el Ecuador Considerando los Cambios de la Estructura Actual. *Rev. Investig. en Energía Medio Ambient. y Tecnol.* **2018**, *3*, 29. [[CrossRef](#)]
45. Tinoco-caicedo, D.L.; Mero-benavides, M.; Santos-torres, M.; Lozano-medina, A.; Blanco-marigorta, A.M. Case Studies in Thermal Engineering Simulation and exergoeconomic analysis of the syngas and biodiesel production process from spent coffee grounds. *Case Stud. Therm. Eng.* **2021**, *28*, 101556. [[CrossRef](#)]
46. Miar Naeimi, M.; Eftekhari Yazdi, M.; Reza Salehi, G. Energy, exergy, exergoeconomic and exergoenvironmental analysis and optimization of a solar hybrid CCHP system. *Energy Sources Part A Recovery Util. Environ. Eff.* **2019**, 1–21. [[CrossRef](#)]
47. Marques, A.D.S.; Carvalho, M.; Lourenço, A.B.; dos Santos, C.A.C. Energy, exergy, and exergoeconomic evaluations of a micro-trigeneration system. *J. Braz. Soc. Mech. Sci. Eng.* **2020**, *42*, 324. [[CrossRef](#)]
48. Cavalcanti, E.J.C.; Carvalho, M.; da Silva, D.R.S. Energy, exergy and exergoenvironmental analyses of a sugarcane bagasse power cogeneration system. *Energy Convers. Manag.* **2020**, *222*, 113232. [[CrossRef](#)]
49. Cavalcanti, E.J.C. Energy, exergy and exergoenvironmental analyses on gas-diesel fuel marine engine used for trigeneration system. *Appl. Therm. Eng.* **2021**, *184*, 116211. [[CrossRef](#)]
50. Wang, J.; Chen, Y.; Lior, N. Exergo-economic analysis method and optimization of a novel photovoltaic/thermal solar-assisted hybrid combined cooling, heating and power system. *Energy Convers. Manag.* **2019**, *199*, 111945. [[CrossRef](#)]
51. Ghaebi, H.; Parikhani, T.; Rostamzadeh, H. A novel trigeneration system using geothermal heat source and liquefied natural gas cold energy recovery: Energy, exergy and exergoeconomic analysis. *Renew. Energy* **2018**, *119*, 513–527. [[CrossRef](#)]

**Disclaimer/Publisher's Note:** The statements, opinions and data contained in all publications are solely those of the individual author(s) and contributor(s) and not of MDPI and/or the editor(s). MDPI and/or the editor(s) disclaim responsibility for any injury to people or property resulting from any ideas, methods, instructions or products referred to in the content.